JOURNAL OF AGRICULTURAL AND FOOD CHEMISTRY

Plant P5C Reductase as a New Target for Aminomethylenebisphosphonates

GIUSEPPE FORLANI,*,† SAMUELE GIBERTI,† ŁUKASZ BERLICKI,‡ DAVIDE PETROLLINO,† AND PAWEŁ KAFARSKI‡

Department of Biology & Evolution, University of Ferrara, Via L. Borsari 46, I-44100 Ferrara, Italy, and Department of Bioorganic Chemistry, Faculty of Chemistry, Wrocław University of Technology, Wybrzeże Wyspiańskiego 27, PL50-370 Wrocław, Poland

A series of *N*-substituted derivatives of aminomethylenebisphosphonic acid were evaluated as potential inhibitors of δ^1-pyrroline-5-carboxylate reductase (EC 1.5.1.2), the enzyme that catalyzes the last step in proline biosynthesis, partially purified from *Arabidopsis thaliana* suspension cultured cells. At millimolar concentrations, three compounds out of 26 were found to interfere with the catalytic mechanism. One of them, namely, 3,5-dichloropyridyl-aminomethylenebisphosphonic acid, retained such inhibitory activity in the micromolar range. Kinetic analyses ruled out the possibility that the inhibition could simply rely upon the chelating properties of bisphosphonates and showed mechanisms of a noncompetitive type against NADH and an uncompetitive type against δ^1-pyrroline-5-carboxylic acid, with K_I values of 199 ± 6 and 10.3 ± 1.5 μM, respectively. A computer-aided docking analysis, performed on the basis of the crystal structure of the enzyme from *Streptococcus pyogenes*, suggested that this phosphonate may interact with amino acid residues near the binding site of δ^1-pyrroline-5-carboxylic acid, thus blocking the substrate in a pocket and preventing its interaction with NADH. Because in higher plants the step catalyzed by δ^1-pyrroline-5-carboxylate reductase is shared by all pathways leading to proline synthesis, such a compound may represent a lead structure to be exploited for the design of new substances endowed with herbicidal activity.

KEYWORDS: Pyridyl derivatives of aminomethylenebisphosphonic acid; P5C reductase; proline synthesis; docking analysis; amino acid biosynthesis inhibitors as herbicides

INTRODUCTION

Modern agrochemicals should have a favorable combination of properties, including high levels of herbicidal activity, low application rates, crop tolerance, and low levels of toxicity to mammals. Moreover, increasing public concern for the environmental pollution deriving from agricultural practice strictly requires that such xenobiotics are endowed with low recalcitrancy, thus being rapidly mineralized by the soil microflora. Intensive efforts have been undertaken in the last decades to discover new compounds with favorable environmental and safety features to selectively control weeds. Recently, this aim has been pursued with new strategies, switching from the classical testing of chemicals for efficacy on whole plants toward either the use of in vitro assays against a given molecular target (e.g., *1*, *2*) or a proteomic/metabolomic approach to rapidly identify the unknown mode of action of a given compound endowed with biological activity (e.g., *3*, *4*). Among these substances, the most remarkable examples to date are provided by a naturally occurring glutamate analogue, phosphinothricin (PPT) (*5*), and a synthetic inhibitor of the shikimate pathway enzyme 5-*enol*-pyruvyl-shikimate-3-phosphate (EPSP) synthase (EC 2.5.1.19), glyphosate (*6*). Both compounds belong to the family of aminoalkylphosphonic acids, structural analogues of amino acids in which the carboxylic group is replaced by a phosphonic or related moiety. This group resembles the tetrahedral transition state of several enzymatic reactions, particularly amide bond formation and hydrolysis. Notwithstanding their significant differences including size, shape (flat CO_2H vs tetrahedral PO_3H_2), and acidity (pK difference of at least 3 units), several enzymes are thus apparently unable to discriminate between carboxylic and phosphonic function for what concerns binding to active sites. In several instances, the structural antagonism between amino acids or their biosynthetic intermediates and the phosphonic counterparts results in inhibition of enzyme activity (*7*, *8*).

PPT acts by inhibiting the key enzyme in ammonia assimilation, glutamine synthetase (GS) (EC 6.3.1.2). This rapidly leads to ammonia accumulation and glutamate depletion, which act in concert to cause plant death (*9*). However, its use is limited because of lack of selectivity. Resistant genetically modified

* To whom correspondence should be addressed. Fax: (39)0532-249761. E-mail: flg@unife.it.
† University of Ferrara.
‡ Wrocław University of Technology.

10.1021/jf0701032 CCC: $37.00
Published on Web 05/03/2007

varieties were indeed developed during recent years (*10*), but at least in Europe, public disfavor toward the use of transgenic crops restrains these results. To improve the weed management potential of such nonselective herbicides, the synthesis of a great number of analogues of the active molecules and their screening for selective forms have been reported (*11*, *12*).

With the aim to identify new active principles, we previously evaluated a series of *N*-pyridyl derivatives of aminomethylenebisphosphonic acid (AMBPA), most of which exerted remarkable phytotoxic effects at both the plant and the cell culture levels (*13*, *14*). Some of them were found to act by interfering with aromatic metabolism at the level of the first enzyme in the shikimate pathway, 3-deoxy-D-arabino-heptulosonate-7-phosphate synthase (EC 4.1.2.15) (*15*, *16*). Some others were indeed shown to inhibit GS, although with lower efficiency than PPT (*17*, *18*). Upon the basis of these results, a structure−activity relationship analysis allowed us to hypothesize structural requirements either to maintain or to enhance such capabilities (*19*).

Proline production is needed in plants for protein and cell wall biosynthesis. In addition, many higher plants transiently accumulate huge intracellular levels of free proline to cope with hyperosmotic stress (*20*), as well as in response to the imposition of a wide range of biotic and abiotic stresses (*21*). The synthesis of this amino acid also seems to play a regulative role promoting seed germination (*22*) and is required during floral development and pollen tube growth (*23*). Thus, the enzymes involved in the anabolic pathway would be greatly attractive as potential targets for new herbicides. However, two metabolic routes leading to proline synthesis have been found in vascular plants. Under normo-osmotic conditions and nitrogen availability, proline is produced mainly through ornithine, an intermediate in arginine biosynthesis, whereas under hyperosmotic stress and nitrogen starvation it is synthesized directly from glutamate (*24*). The presence of multiple pathways would hamper the attempt to induce proline starvation through the inhibition of the first enzymes, which are supposed to catalyze the rate-limiting steps, allowing the plant to recover. This nothwithstanding, because the two pathways share the last reaction, catalyzed by a δ^1-pyrroline-5-carboxylate (P5C) reductase (EC 1.5.1.2) (*24*), this goal might be achieved through the development of a specific inhibitor for such an enzyme. However, at least to our knowledge, no inhibitors of P5C reductase were reported in the literature so far.

Here, we report the results of a screening of 26 aminobisphosphonates for the ability to inhibit P5C reductase, isolated from *Arabidopsis thaliana* cultured cells. Three of them were found to interfere with the catalytic mechanism in the millimolar range, and one retained this capability at micromolar concentrations. A thorough kinetic evaluation coupled with a computer-assisted docking analysis allowed us to hypothesize its mechanism of action at the molecular level, one that could provide the basis for the future design of new inhibitors.

MATERIALS AND METHODS

Chemicals. Unless otherwise indicated, chemicals were purchased from Sigma Chemicals (St. Louis, MO) and were of analytical grade. *N*-Substituted derivatives of AMBPA (**Figure 1**) were obtained by reacting the corresponding amine with equimolar quantities of ethyl orthoformate and triethyl phosphite, followed by acidic hydrolysis as previously described (*14*). DL-P5C was synthesized by the periodate oxidation of *δ*-*allo*-hydroxylysine and purified by cation-exchange chromatography on a Dowex AG50 (200−400 mesh) column, as described (*25*, *26*).

Plant Material, Cell Culture Induction, and Growth Conditions. Seeds of *A. thaliana* Heyn., ecotype Columbia, were surface-sterilized and allowed to germinate onto an agarized MS medium containing 30 g L^{-1} sucrose and 0.5 mg L^{-1} of both 2.4D and 6.BAP. Calluses were amplified for 4 months, and then, friable material was transferred into liquid medium. Cultures were incubated at 24 ± 1 °C on a rotary shaker (100 rpm) under dim (<50 μmol m^{-2} s^{-1}) light. After 6 months of subculturing, a well-dispersed, homogeneous culture was obtained. Subcultures were made every 10 days by transferring 30 mL aliquots of the suspension to 100 mL of fresh medium in 500 mL Erlenmeyer flasks.

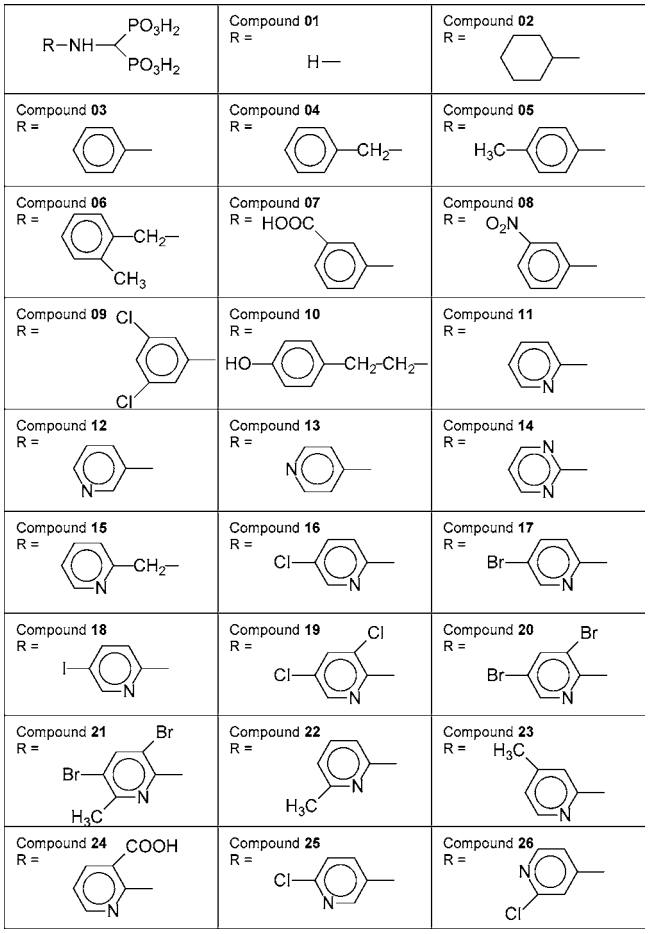

Figure 1. Derivatives of AMBPA (compound **1**) evaluated as possible inhibitors of plant P5C reductase.

P5C Reductase Purification. Cells harvested in the early stationary phase of growth were resuspended in 2 mL g^{-1} of ice cold extraction buffer [50 mM Tris-HCl, pH 7.4, containing 0.5 mM dithiothreitol (DTT) and 0.5 mM ethylenediaminetetraacetic acid (EDTA)] and homogenized for 10 min in a mortar equilibrated on ice with 1 g (g cells)$^{-1}$ quartz sand. All subsequent operations were carried out at 0−4 °C. Following centrifugation at 12000*g* for 15 min, the resulting supernatant was added with solid ammonium sulfate up to 50% of saturation. Precipitated proteins were pelleted by centrifugation, resuspended in a minimal amount of extraction buffer, and desalted by passage through a Bio-Gel P6DG (Bio-Rad) column. The sample was then loaded onto a DEAE-Sephacel (Pharmacia) column equilibrated with extraction buffer. Unretained material was buffer-exchanged against column buffer (50 mM Na bicarbonate, pH 10, containing 0.5 mM DTT and 0.5 mM EDTA) and loaded onto a second DEAE-Sephacel column equilibrated with the same buffer. Proteins were eluted at a constant flow of 1 mL min^{-1} with a linear gradient from 0 to 250 mM NaCl in column buffer (400 mL), while collecting 5 mL fractions. Active fractions were pooled, column-desalted as above against extraction buffer, and stored at 4 °C until used for biochemical determinations. Under these conditions, P5C reductase activity was found to be stable for at least 2 months.

Enzyme Assays. The physiological, forward reaction of P5C reductase was routinely measured by following the P5C-dependent

Table 1. Partial Purification of P5C Reductase from *A. thaliana* Heyn. Suspension Cultured Cells[a]

step	protein (mg)	activity (nkat)	specific activity (nkat mg^{-1})	purification (fold)	yield (%)
1. Crude extract	732.3	585	0.799	1	100
2. 0–50% ammonium sulfate fraction	466.4	511	1.115	1.4	87.4
3. DEAE-Sephacel pH 7.5, flow-through	129.4	406	3.14	3.9	69.4
4. DEAE-Sephacel pH 10.0, pool	5.25	251	47.8	59.8	42.9

[a] Results presented are for a typical purification starting from 100 g (fresh weight) of suspension cultured cells harvested in the early stationary phase of growth.

oxidation of NADH. The assay mixture contained 100 mM Tris-HCl buffer, pH 8.0, 0.1 mM $MgCl_2$, 2 mM DL-P5C, and 0.25 mM NADH, in a final volume of 1 mL. A limiting amount of enzyme (0.05−0.25 nkat) was added to the prewarmed mixture, and the decrease in absorbance was determined at 35 °C for up to 10 min by continuous monitoring of the sample at 340 nm against blanks from which P5C had been omitted. The activity was determined from the initial linear rate, with the assumption of an extinction coefficient of 6220 M^{-1} cm^{-1}. Because several pyridyl derivatives of AMBPA were found to strongly absorb light in the UV-B range, their addition at the millimolar level to the reaction mixture can interfere with the above protocol. To overcome such a drawback, an alternative assay method was used that follows P5C utilization. After the addition of the enzyme to the prewarmed mixture in a final volume of 1.2 mL, 100 μL aliquots were withdrawn every 40 s, added sequentially with 50 μL of 4.5 M Na acetate and 1 mL of 0.15% (w/v) ninhydrin in acetic acid, and incubated 10 min at 55 °C. The residual concentration of P5C was estimated from the resulting absorbance at 535 nm on the basis of a molar extinction coefficient of 4600 M^{-1} cm^{-1} (*26*). The protein concentration was determined by the method of Bradford (*27*), using bovine serum albumin as the standard.

Enzyme Inhibition and Kinetic Analysis. P5C reductase inhibition was evaluated by adding to the reaction mixture an appropriate dilution of a 20 mM solution of a given inhibitor, brought to pH 7.4 with KOH, so as to obtain a final concentration of 1, 0.5, or 0.2 mM. At least three measurements were performed for each dose. Active compounds were tested in the micromolar range. The concentrations causing 50% inhibition (I_{50}) of P5C reductase activity were estimated utilizing the linear regression equation of enzyme activity values, expressed as a percentage of untreated controls, plotted against the logarithm of inhibitor concentration. Confidence limits of I_{50} values were computed according to ref *28*. For kinetic evaluations, the enzyme was assayed in the presence of increasing concentrations of compound **9** by varying those of the substrates. Unvariable substrates were fixed at the same levels than in standard assay. The concentration for the variable substrate ranged from 0.07 to 0.28 mM NADH and from 0.2 to 1 mM L-P5C. At least eight doses were evaluated for each substrate, at no less than triplicate. In the case of P5C (uncompetitive inhibition), K_i values were estimated from Lineweaver−Burk plots of activity, on the basis of the corresponding lowering in the apparent K_M value; five inhibitor concentrations, ranging from 0.2- to 1.5-fold the I_{50} value, were tested. In the case of NADH (noncompetitive inhibition), K_i values were estimated from Dixon plots of activity by evaluating the effect of four inhibitor levels, ranging from 0.6- to 3-fold the I_{50} value, in the presence of 10 substrate concentrations. To confirm the inhibitory mechanism, NADPH was also tested as the variable substrate, at concentrations ranging from 12 to 60 μM. Reported data are means ± standard errors of the mean (SEM) over results obtained with different inhibitor or substrate concentrations, respectively.

Binding Pattern Analysis of the Active Compound to P5C Reductase. The crystal structure of the enzyme complexed with proline from *Streptococcus pyogenes* (*29*), obtained from Protein Data Bank (*30*) (refcode 2AMF), was used as a starting point for all calculations, and residue numbering is according to this structure. The hydrogen atoms were added using Insight 2000 program (Accelrys) (*31*), and the protonation states of the amino acid side chain residues were set up for pH 7.0. Molecular mechanics calculations were performed using Discover program with cff97 force field and conjugate gradient minimizer (*32*). Minimizations were done up to energy change 0.01 kcal mol^{-1}. Optimized structures were scored using LUDI functions from LUDI program (*33*, *34*) derived from the Insight package. The SCORE_ALL value describes all interactions between inhibitor and enzyme, whereas the HB_SCORE value describes hydrogen bonds and the LIPO_SCORE value describes lipophilic interactions.

RESULTS AND DISCUSSION

Purification of P5C Reductase from *A. thaliana* Cultured Cells. Aiming at the evaluation of possible inhibitors for the enzyme that catalyzes the last step in proline biosynthesis, the model plant *A. thaliana* was selected as the protein source because its genome has been completely sequenced, and facilities are available for a thorough genetic analysis (*35*). Upon the basis of these data, only one gene coding for a P5C reductase is present in thale cress, contrary to other higher plants, in which the occurrence of multiple enzyme forms was reported (*36*). A proper evaluation could in fact be hampered by the presence of isozymes with different sensitivity. To obtain reliable results, inhibition studies should be also performed with homogeneous enzyme preparations. The residual presence of activities able to make use of the same substrates or further metabolize the products may lead to experimental artifacts or at least interfere heavily with enzyme assay. This is quite true for enzymes involved in proline metabolism. In crude extract and in the presence of nonlimiting P5C concentrations, the NAD^+ produced by P5C reductase would be immediately reduced by the activity of P5C dehydrogenase (EC 1.5.1.12) (*25*). Moreover, some available assay methods may be unfeasible, because they measure partial or reverse—thus nonphysiological—reactions. This is the case for one of the most common protocols to measure P5C reductase, which follows the proline-dependent reduction of NAD^+ at high pH values (e.g., *29*, *37*). However, compounds able to interfere with enzyme activity under such assay conditions might be scarcely effective on the whole forward reaction or vice versa. To avoid such drawbacks, the enzyme was assayed by protocols that measure the full, forward reaction, and biochemical evaluations were carried out with purified preparations. Because of the small size of *Arabidopsis* seedlings, the protein was isolated from suspension cultured cells, after a well-dispersed culture had been obtained starting from calluses induced from germinating seeds. Following an initial enrichment by ammonium sulfate fractionation, the remarkably high isoelectric point (8.48), calculated for *A. thaliana* P5C reductase on the basis of the predicted amino acid sequence (*35*), allowed us to set up a highly resolving, double-step protocol by anion exchange chromatography. The maximal specific activity observed corresponded to a 60-fold purification, with a yield of about 50% of the initial activity (**Table 1**). Even if not homogeneous, since several protein bands were still evident in sodium dodecyl sulfate−polyacrylamide gel electrophoresis patterns (data not shown), preparations were apparently devoid of any other enzymatic activity able to either oxidize NADH/reduce NAD^+ or use P5C as a substrate. The P5C dehydrogenase activity was below the sensitivity level of the assay method (0.05 pkat mL^{-1}; *25*). Although it was cloned in

the early nineties (*38*), to our knowledge, neither *A. thaliana* P5C reductase has been purified to date nor its biochemical properties have been evaluated thoroughly. The partially purified protein was thus characterized with respect to kinetic parameters, to ensure nonlimiting assay conditions during the subsequent analyses. Apparent affinity constants were 0.39 ± 0.02 and 0.23 ± 0.01 mM for L-P5C and NADH, respectively. NADPH also was found to be used as a substrate, with an even higher affinity (K_M value of 24 ± 1 μM). However, $V_{maxNADPH}$ was about sixfold lower than $V_{maxNADH}$; thus, the former dinucleotide was routinely used. The enzyme retained maximal activity over a broad range from pH 7.2 to pH 8.6. Divalent cations were neither required nor stimulated activity (results not presented). Notwithstanding this, a low concentration of $MgCl_2$ was included in the assay mixture, according to most previously described protocols (e.g., *37*, *39*).

P5C Reductase Inhibition by Aminobisphosphonates. The ability of several substituted AMBPA derivatives to interfere with the catalytic mechanism of P5C reduction was then evaluated with the partially purified enzyme under the optimal assay conditions identified this way. Preliminary experiments seemed to account for a general capacity of these compounds for inhibiting P5C reductase when added to the assay mixture at millimolar levels. However, proper checks pointed out that such a behavior was in fact an experimental artifact deriving from the ability of most of them to strongly absorb light in the UV-B range (data not shown). This resulted in an apparent decrease of the molar extinction coefficient for NADH, turning into a specious inhibition of its enzymatic oxidation. To avoid such an interference, the assay was repeated with a lower amount of aminophosphonates (0.2 mM). Moreover, the molar absorptivity for the substrate was experimentally determined in the presence of the same level of each compound, and data were corrected accordingly. Results, summarized in **Table 2**, showed that only three compounds out of 26 were indeed able to significantly reduce the catalytic rate of *A. thaliana* P5C reductase. To obtain further support, a different assay protocol was set up, one that follows P5C utilization instead of NADH oxidation. Its availability allowed us to overcome interferences in the UV-B range and to increase phosphonate concentration. Data, also shown in **Table 2**, were consistent with those obtained with the former method in the case of compounds **9** and **21**, whereas data did not confirm the inhibitory properties of compound **22**. AMBPA itself (compound **1**) was slightly effective.

Because several bisphosphonic acids show remarkable chelating properties (*13*, *15*), this effect might simply rely upon ion sequestration. Enzyme activity neither required nor was stimulated by cation addition. Nevertheless, the compounds could strip away bound metal still retained by the protein after the purification procedure. To exclude an inhibition solely on the basis of cation chelation and to obtain more reliable quantitative data, thale cress P5C reductase was assayed in the presence of each of the three compounds that significantly reduced the physiological reaction, in the range from 0.010 to 5 mM. In the case of metal chelation, no inhibition is expected to occur until the concentration of the compound is lower than a threshold, above which a complete suppression of enzyme activity is found (*16*). This was not the case, since all phosphonates progressively inhibited P5C reductase (**Figure 2**). Moreover, the same levels of ethylenediaminetetraacetic acid, a well-known substance able to chelate divalent cations, were found completely ineffective (not shown). The concentrations causing 50% inhibition (I_{50}) were equal to 44 ± 15, 0.077 ± 0.011, and 0.30 ± 0.03 mM for compounds **1**, **9**, and **21**, respectively. Compound **1** has thus to be regarded as poorly

Table 2. Inhibition of Thale Cress P5C Reductase by Substituted Derivatives of AMBPA

	P5C utilization assay method[a]		NADH oxidation assay method[b]	
compound	% of control ± SE	*n*	% of control ± SE	*n*
none	100.0 ± 3.0	17	100.0 ± 0.9	19
1 (AMBPA)	84.6 ± 8.8*	4	106.1 ± 5.5	4
2	93.8 ± 6.1	3	108.0 ± 4.7	4
3	114.1 ± 3.2	3	98.3 ± 4.5	4
4	100.2 ± 5.2	3	98.5 ± 5.1	4
5	98.2 ± 1.3	3	109.5 ± 6.0	4
6	96.9 ± 3.5	3	108.8 ± 4.7	4
7	92.4 ± 5.0	3	95.0 ± 4.3	4
8	96.4 ± 1.6	3	102.5 ± 4.8	4
9	28.0 ± 3.2***	3	37.7 ± 6.8***	4
10	94.4 ± 6.9	3	105.1 ± 2.1	4
11	104.1 ± 7.7	3	113.5 ± 5.7	4
12	102.0 ± 3.2	3	108.8 ± 2.9	4
13	100.8 ± 2.4	3	115.0 ± 2.2	4
14	91.7 ± 6.4	3	110.0 ± 3.8	4
15	92.9 ± 5.5	3	118.0 ± 4.5	4
16	92.4 ± 7.3	3	101.4 ± 10.0	4
17	100.3 ± 4.6	3	104.4 ± 4.5	4
18	89.9 ± 7.9	4	105.8 ± 4.3	4
19	97.0 ± 1.3	3	104.8 ± 4.1	4
20	99.8 ± 4.7	3	92.0 ± 1.2	4
21	54.8 ± 7.7***	3	66.1 ± 7.8***	4
22	103.1 ± 1.0	3	88.7 ± 13.6*	4
23	105.5 ± 4.0	3	106.0 ± 7.3	4
24	94.1 ± 5.9	3	96.3 ± 4.6	4
25	94.9 ± 6.9	3	99.4 ± 2.5	4
26	97.9 ± 3.1	3	91.2 ± 2.8	4

[a] Activity was evaluated by measuring the disappearance of P5C from the reaction mixture, as detailed in the Materials and Methods, in the presence of AMBPA and its derivatives at a concentration of 0.5 mM. Each treatment was carried out at least three times, as indicated, and values were expressed as the percentage of untreated controls. Significant differences between a given treatment and controls are marked. *, $P < 0.10$; **, $P < 0.05$; and ***, $P < 0.01$. [b] P5C reductase activity was also measured in the presence of AMBPA and its derivatives at a concentration of 0.2 mM by continuously monitoring the P5C-dependent oxidation of NADH at 340 nm. However, because several compounds strongly absorb light in the UV-B range, their presence in the millimolar range can interfere with the assay. To avoid artifacts, the molar extinction coefficient of NADH in the presence of the above level of each compound was experimentally determined, and data were corrected accordingly. Replication and statistical analysis were as in the previous case.

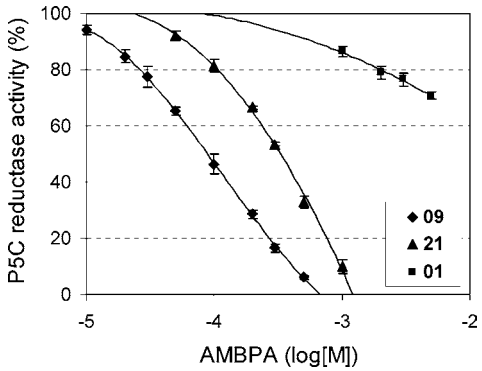

Figure 2. Effect of increasing concentrations of active compounds upon the catalytic rate of P5C reductase isolated from *A. thaliana* cultured cells. Data, expressed as percentage of untreated controls, are means ± SD over at least three replications. The linear regression equations of enzyme activity values plotted against the logarithm of inhibitor concentration allowed the calculation of I_{50} values, which were equal to 44 ± 15, 0.077 ± 0.011, and 0.30 ± 0.03 mM for compounds **1**, **9**, and **21**, respectively.

effective, and also, compound **21** requires very high concentrations to be suppressive. On the contrary, the inhibition brought about by compound **9** is noteworthy, being almost equipotent to that of substituted PPTs inhibiting plant GSs (I_{50} in the range from 30 to 40 μM; *12*) and equal to that of the EPSP synthase inhibitor glyphosate (I_{50} of about 100 μM; *16*).

Mechanism of Action. To obtain some information concerning the inhibitory mechanism, a thorough kinetic analysis was then carried out for the most effective derivative **9**. Results (**Figure 3**) accounted for an inhibition of noncompetitive type with respect to NADH and uncompetitive against P5C. Because in vivo NADPH could be used as an alternative substrate, enzyme inhibition was also determined by replacing NADH with the phosphorylated dinucleotide. Data, summarized in panel **B** of **Figure 3**, confirmed the results obtained with NADH. In uncompetitive inhibition, the inhibitor binds to the active site only after the substrate has bound, whereas in noncompetitive inhibition two independent binding sites are present. Data thus suggest that compound **9** interacts with the enzyme differently and independently from the dinucleotide but following the formation of a P5C−enzyme complex. This implies that substrate binding in plant P5C reductase active site is of sequential character [P5C binds before NAD(P)H], a fact that is consistent with recent data describing the crystal structure at 2 Å resolution of P5C reductase from two human pathogens, *Neisseria meningitides* and *S. pyogenes*. A surface rendering of the active center of the structure of the enzyme from *S. pyogenes* complexed with NADPH showed that, upon binding of the coenzyme, the entrance to the active center cavity is effectively blocked, leaving only a small opening that is insufficient to allow P5C to pass (*29*). A similar structure was described thereafter for the human enzyme (*39*). This strongly supports the hypothesis that P5C binds first, followed by NAD(P)H. From a quantitative point of view, the calculated K_i values were 10.3 ± 1.5, 199 ± 6, and 230 ± 11 μM with respect to P5C, NADH, and NADPH. As a term of comparison, an almost identical value was found for the inhibition of maize EPSP synthases by glyphosate with respect to shikimate-3-phosphate, which is also uncompetitive. However, the K_i against the other substrate phosphoenolpyruvate, of competitive type, was three orders of magnitude lower than that herein calculated with respect to NADH (*41*). The finding that the inhibition is uncompetitive against P5C implies that the V_{max}' (V_{max} in the presence of the inhibitor) will always be equal to V_{max} divided by $1 + I/K_i$, regardless of the substrate concentration. On the contrary, a competitive inhibitor will be displaced by an increase in substrate concentration. Because enzyme inhibition in vivo always causes an increase in substrate pool that can significantly relieve inhibition, competitive inhibitors are usually much less effective in vivo than they are in vitro (*42*). Thus, compound **9** is probably going to be more effective inside the cell than similar inhibitors working competitively.

Computer-Aided Analysis of Inhibitor Binding to P5C Reductase. The number of substituted AMBPA derivatives that was found active against the enzyme from thale cress is too small to allow a reliable structure−activity relationship analysis. To shed some further light on the mode of action at the molecular level and allow hypothesizing structural requirements either to maintain or to enhance the inhibitory properties, a docking analysis of the most effective compound **9** to the active site of the enzyme was performed. Because no crystal structure is available for any plant P5C reductase, that of the enzyme from *S. pyogenes* was used. Being quite distant on the evolutionary scale, these proteins are expected to show moderate similarity. An alignment of the deduced amino acid sequences (**Figure 4**) indeed pointed out a moderate degree of conservation, with 33% identities, 56% conserved residues, and 3% gaps. However, the sequences showed similarity over their entire

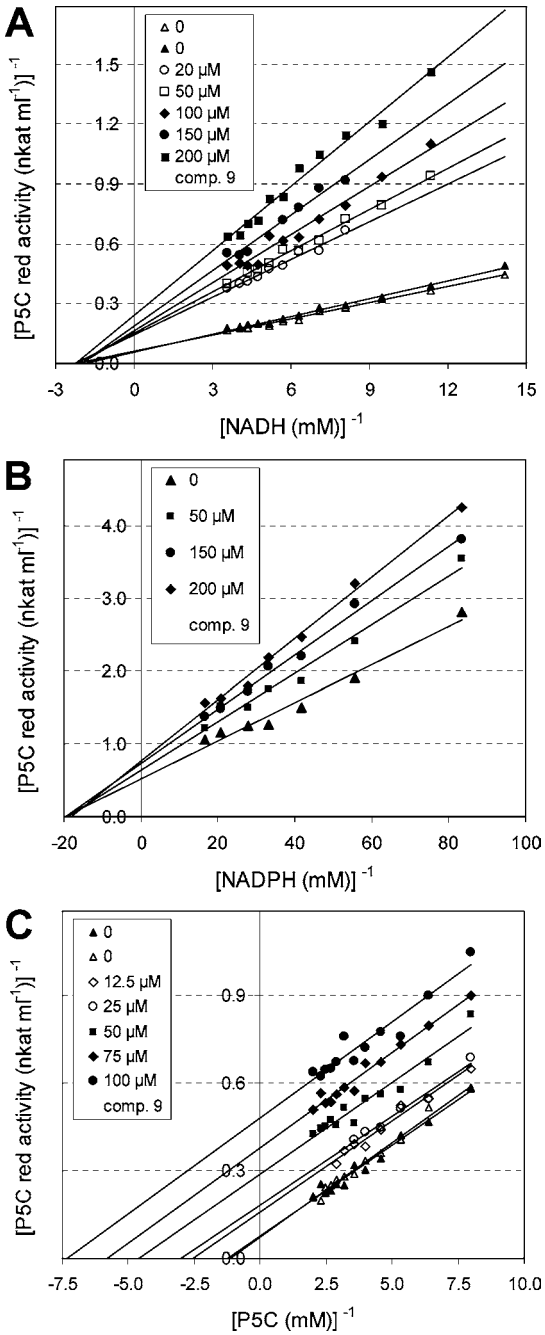

Figure 3. Kinetic analysis of P5C reductase inhibition by compound **9**. The enzyme partially purified from *A. thaliana* cultured cells was incubated in the presence of increasing inhibitor concentrations at varying given substrate levels. Lines converging to the *x*-axis in Lineweaver–Burk plot accounted for an inhibition of noncompetitive type against NADH (**A**; K_i = 199 ± 6 μM), whereas parallel lines showed an inhibition of uncompetitive type with respect to P5C (**C**). Replotting of data in panel **C** as a Dixon plot resulted in a K_i value of 10.3 ± 1.5 μM. A multiple regression analysis showed in all cases a high significance level ($P < 0.00$) with respect to both variables (inhibitor and substrate concentration). A noncompetitive inhibition type was obtained with NADPH also, which can be used as a substrate with an even higher affinity but yielding a six-fold lower maximal rate (**B**). In this case, data accounted for a K_i value of 230 ± 11 μM.

```
S_pyogenes ----------MKIGIIGVGKMASAIIKGLKQT----PHELIISGSSLERSKEIAEQLALP 46
A_thaliana MEILPIPAESFKVGFIGAGKMAESIARGVVASGVLPPNRICTAVHSNLNRRDVFESFGVN 60
                     :*:*:**.****.:* :*:  :    *:.:  :  *  . ::: *.:.:

S_pyogenes YAMSHQDLIDQVDLVILGIKPQLFETVLKPLHFKQP----IISMAAGISLQRLATFVGQD 102
A_thaliana VFSTSEEVVKESDVVIFSVKPQVVKKAVTELKSKLSKNKILVSVAAGIKLNDLQEWSGQD 120
             : :::::.: *:**:.:***:.:::.:. *: * .    ::*:****.*: *  : ***

S_pyogenes LPLLRIMPNMNAQILQSSTALTGNALVSQELQARVRDLTDSFGSTFDISEKDFDTFTALA 162
A_thaliana R-FIRVMPNTPAAVGEAASVMSLGTGATEEDGAIVAMLFGAVGKILKADEKMFDAVTGLS 179
            ::*:***  * : ::::.:: .: .::*  * *  * .:.*. :. .** **:.*.*:

S_pyogenes GSSPAYIYLFIEALAKAGVKNGIPKAKALEIVTQTVLASASNLKTSSQSPHDFIDAICSP 222
A_thaliana GSGPAYIFLAIEALADGGVAAGLPRELALSLASQTVLGAATMVSKTGKHPGVLKDDVTSP 239
           **.****:* *****..**  *:*:  **.:.:****.:*: :..:.: *  : * : **

S_pyogenes GGTTIAGLMELERLGLTATVSSAIDKTIDKAKSL--- 256
A_thaliana GGTTIAGVHELEKGSFRATLMNAVVAAAKRSRELSQS 276
           *******: ***: .: **: .*:  : .::::.*
```

Figure 4. Sequence alignment of *A. thaliana* and *S. pyogenes* P5C reductases. ClustalW (1.83) analysis was performed with the deduced amino acid sequences (accession numbers NC003076 and Q9A1S9, respectively). Key: –, gaps introduced to maximize alignment; *, identical residues; :, highly conserved; and ., conserved residues. Lys10, Met11, and Ser221, which were predicted to interact with compound **9**, are highlighted.

Table 3. LUDI Score Values for Selected AMBPA Derivatives[a]

compound	SCORE_ALL	HB_SCORE	LIPO_SCORE
1	197	329	14
9	511	325	358
19	430	256	346
21	389	245	316
26	417	282	307

[a] The LUDI_1 scoring function from LUDI program (*33*, *34*) from Insight molecular modeling program package (*31*) was used.

lengths, a fact that is suggestive of a similar three-dimensional structure. Moreover, residues predicted to interact with the bisphosphonate (Lys10, Met11, and Ser221) were found to be identical in the two enzymes. Thus, results obtained with the bacterial enzyme could also be useful for a better understanding of the interaction with the plant protein. A proline−enzyme complex (PDB code 2AMF) was used for calculations, as kinetic measurements suggested that the inhibitor binds to the active site after the substrate. The obtained structure of the compound **9**−proline−P5C reductase complex (**Figure 5A**) showed that the bisphosphonate moiety interacts favorably with the enzyme forming four hydrogen bonds with Lys10, Met11, and Ser221. The aromatic part of compound **9** fits very tightly to the cavity of the enzyme (**Figure 5B**), and lipophilic interactions between the inhibitor and the protein were also observed. In such a way, the bisphosphonate molecule blocks P5C in the active site (**Figure 5C**), a fact that is consistent with kinetic data showing an inhibition of uncompetitive type.

To quantitatively evaluate inhibitor−protein interactions, the LUDI scoring function, which by definition correlates with pK_i, was applied. Moreover, two components of this function, namely, HB_SCORE and LIPO_SCORE (*34*), which, respectively, describe the contribution of hydrogen bonds and lipophilic interactions in ligand binding, were calculated. The values obtained for compound **9** (**Table 3**) proved that both types of interactions are of importance for complex stability. The evaluation of optimized complexes of other AMBPA derivatives showed different patterns (**Table 3**). Unsubstituted compound **1** maintained all hydrogen bonds observed with compound **19**, but a significantly reduced SCORE_ALL resulted from the absence of the aromatic ring causing a very low LIPO_SCORE value. Derivatives **19**, **21**, and **26** have similar substituents but in different positions. This causes an altered positioning of the aromatic moiety and the change of the hydrogen bond network. Thus, the LIPO_SCORE of compounds **21** and **26** is similar to that of compound **19**, but the HB_SCORE is significantly reduced, causing lower SCORE_ALL values that are consistent with the lower activity observed (**Table 2**).

Molecular modeling clearly shows that compound **9** binds after P5C and covers the space available for its interaction with the cosubstrate, with the phosphonate located closely to the pyrophosphate moiety of NADH. Thus, taking into account the results from both experiments and calculations, a bulky substituent in position 3 of the aromatic ring is necessarily required but not sufficient for high inhibitory activity.

Conclusions. Several AMBPA derivatives were evaluated for the ability to inhibit the enzyme that catalyzes the last step in proline biosynthesis, P5C reductase. At least two of them were proved to be effective in the micromolar range against the plant protein, representing the first inhibitors of the enzyme described to date. A kinetic analysis of the inhibition brought about by the most powerful compound **9** suggested that this aminobisphosphonate acts by complexing to the active site after P5C binding. A docking analysis based upon the crystal structure of the bacterial enzyme led us to hypothesize that it might interact with amino acid residues near the entrance to the active center cavity, thus blocking P5C in a pocket and preventing its interaction with NAD(P)H. Despite the fact that *A. thaliana* and *S. pyogenes* P5C reductases show a moderate similarity, this would most likely occur also for the plant enzyme. When the crystal structure of the human P5C reductase was compared with those of *S. pyogenes* and *N. meningitides*, although their levels of primary structure similarities are even lower (22−26%), they were indeed found to share a generally similar monomer structure and dimer architecture (*40*).

Being an aromatic chlorinated molecule, and thus most likely endowed with high recalcitrancy, compound **9** itself cannot represent an optimal candidate as a new active principle. However, data herein described, coupled with the results of a further analysis of the inhibitor's positioning inside the protein, currently in progress, should allow us to hypothesize steric and electronic requirements either to maintain or to enhance this inhibitory capability. Because the step catalyzed by P5C reductase is shared in plants by both pathways leading to proline biosynthesis, the computer-aided design of other inhibitors could

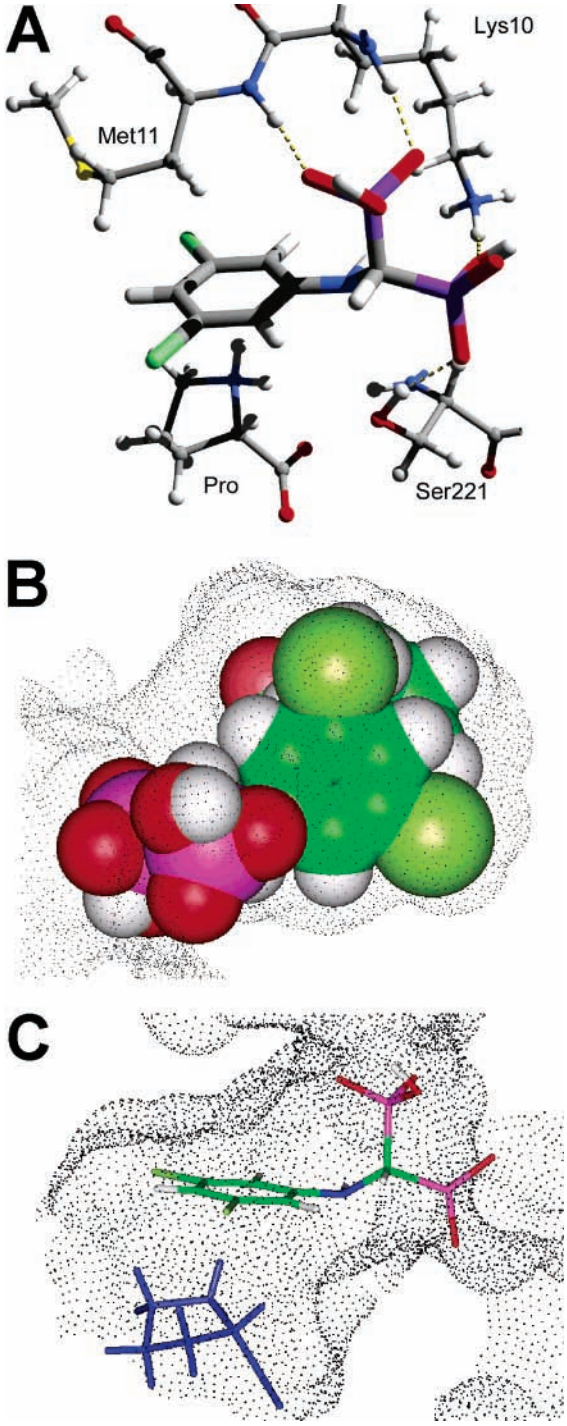

Figure 5. Putative positioning of compound **9** inside the active site of P5C reductase: (**A**) side view with hydrogen bonds showed (dashed lines), (**B**) top view with marked surface of the enzyme, and (**C**) side view with marked surface. In all panels, proline (the product of the reaction) is located below the inhibitor.

lead in the future to the development of new active ingredients endowed with herbicidal activity.

ACKNOWLEDGMENT

The calculations were carried out using hardware and software resources (including the Accelrys programs) of the Supercomputing and Networking Centre in Wrocław.

LITERATURE CITED

(1) Doyle, J. R.; Burnell, J. N.; Haines, D. S.; Llewellyn, L. E.; Motti, C. A.; Tapiolas, D. M. A rapid screening method to detect specific inhibitors of pyruvate orthophosphate dikinase as leads for C-4 plant-selective herbicides. *J. Biomol. Screening* **2005**, *10*, 67−75.

(2) Vicentini, C. B.; Guccione, S.; Giurato, L.; Ciaccio, R.; Mares, D.; Forlani, G. Pyrazole derivatives as photosynthetic electron transport inhibitors: New leads, and structure-activity relationship. *J. Agric. Food Chem.* **2005**, *53*, 3848−3855.

(3) Grossmann, K. What it takes to get a herbicide's mode of action. Physionomics, a classical approach in a new complexion. *Pest Manage. Sci.* **2005**, *61*, 423−431.

(4) Wheelock, C. E.; Miyagawa, H. The omicization of agrochemical research. *J. Pestic. Sci.* **2006**, *31*, 240−244.

(5) Hoerlein, G. Glufosinate (phosphinothricin), a natural amino acid with unexpected herbicidal properties. *Rev. Environ. Contam. Toxicol*. **1994**, *138*, 73−145.

(6) Baylis, A. D. Why glyphosate is a global herbicide: Strengths, weaknesses and prospects. *Pest Manage. Sci.* **2000**, *56*, 299−308.

(7) Kafarski, P.; Lejczak, B.; Forlani, G. Herbicidally active aminomethylenebisphosphonic acids. *Heteroat. Chem.* **2000**, *11*, 449−453.

(8) Priestman, M. A.; Healy, M. L.; Becker, A.; Alberg, D. G.; Bartlett, P. A.; Lushington, G. H.; Schonbrunn, E. Interaction of phosphonate analogues of the tetrahedral reaction intermediate with 5-enolpyruvylshikimate-3-phosphate synthase in atomic detail. *Biochemistry* **2005**, *44*, 3241−3248.

(9) Evstigneeva, Z. G.; Solov'eva, N. A.; Sidel'nikova, L. I. Methionine sulfoximine and phosphinothricin: A review of their herbicidal activity and effects on glutamine synthetase. *Appl. Biochem. Microbiol.* **2003**, *39*, 539−543.

(10) Tan, S.; Evans, R.; Singh, B. Herbicidal inhibitors of amino acid biosynthesis and herbicide-tolerant crops. *Amino Acids* **2006**, *30*, 195−204.

(11) Inoue, M.; Hiratake, J.; Sakata, K. Synthesis and characterization of intermediate and transition-state analogue inhibitors of γ-glutamyl peptide ligases. *Biosci., Biotechnol., Biochem.* **1999**, *63*, 2248−2251.

(12) Forlani, G.; Obojska, A.; Berlicki, Ł; Kafarski, P. Analogues of phosphinothricin as inhibitors of plant glutamine synthetases. *J. Agric. Food Chem.* **2006**, *54*, 796−802.

(13) Forlani, G.; Kafarski, P.; Lejczak, B.; Wieczorek, P. Mode of action of herbicidal derivatives of aminomethylenebisphosphonic acid. II. Reversal of herbicidal action by aromatic amino acids. *J. Plant Growth Regul.* **1997**, *16*, 147−152.

(14) Kafarski, P.; Lejczak, B.; Forlani, G.; Gancarz, R.; Torreilles, C.; Grembecka, J.; Ryczek, A.; Wieczorek, P. Herbicidal derivatives of aminomethylenebisphosphonic acid. III. Structure-activity relationship. *J. Plant Growth Regul.* **1997**, *16*, 153−158.

(15) Forlani, G.; Lejczak, B.; Kafarski, P. *N*-pyridyl-aminomethylenebisphosphonic acids inhibit the first enzyme in the shikimate pathway, 3-deoxy-D-*arabino*-heptulosonate-7-phosphate synthase. *Pestic. Biochem. Physiol.* **1996**, *55*, 180−188.

(16) Forlani, G.; Lejczak, B.; Kafarski, P. The herbicidally active compound *N*-2-(6-methyl-pyridyl)-aminomethylene-bisphosphonic acid inhibits *in vivo* aromatic biosynthesis. *J. Plant Growth Regul.* **1999**, *18*, 73−79.

(17) Forlani, G.; Lejczak, B.; Kafarski, P. The herbicidally active compound *N*-2-(5-chloro-pyridyl)-aminomethylene-bisphosphonic acid acts by inhibiting both glutamine and aromatic amino acid biosynthesis. *Aust. J. Plant Physiol.* **2000**, *27*, 677−683.

(18) Obojska, A.; Berlicki, Ł; Kafarski, P.; Lejczak, B.; Chicca, M.; Forlani, G. Herbicidal pyridyl derivatives of amino-methylenebisphosphonic acid inhibit plant glutamine synthetase. *J. Agric. Food Chem.* **2004**, *52*, 3337−3344.

(19) Berlicki, Ł; Kafarski, P. The use of molecular modelling for comparison of three possible modes of action of herbicidally active derivatives of aminomethylene-bisphosphonic acid. *Pestic. Biochem. Physiol.* **2002**, *73*, 94−103.
(20) Yoshiba, Y.; Kiyosue, T.; Nakashima, K.; Yamaguchi-Shinozaki, K.; Shinozaki, K. Regulation of levels of proline as an osmolyte in plants under water stress. *Plant Cell Physiol.* **1997**, *38*, 1095−1102.
(21) Hare, P. D.; Cress, W. A. Metabolic implications of stress-induced proline accumulation in plants. *Plant Growth Regul.* **1997**, *21*, 79−102.
(22) Hare, P. D.; Cress, W. A.; van Staden, J. A regulatory role for proline metabolism in stimulating *Arabidopsis thaliana* seed germination. *Plant Growth Regul.* **2003**, *39*, 41−50.
(23) Schwacke, R.; Grallath, S.; Breitkreuz, K. E.; Stransky, E.; Stransky, H.; Frommer, W. B.; Rentsch, D. LeProT1, a transporter for proline, glycine betaine, and γ-amino butyric acid in tomato pollen. *Plant Cell* **1999**, *11*, 377−391.
(24) Kavi Kishor, P. B.; Sangam, S.; Amrutha, R. N.; Sri Laxmi, P.; Naidu, K. R.; Rao, K. R. S. S.; Rao, S.; Reddy, K. J.; Theriappan, P.; Sreenivasulu, N. Regulation of proline biosynthesis, degradation, uptake and trasport in higher plants: Its implications in plant growth and abiotic stress tolerance. *Curr. Sci.* **2005**, *88*, 424−438.
(25) Forlani, G.; Scainelli, D.; Nielsen, E. Δ^1-Pyrroline-5-carboxylate dehydrogenase from cultured cells of potato. Purification and properties. *Plant Physiol.* **1997**, *113*, 1413−1418.
(26) Williams, I.; Frank, L. Improved chemical synthesis and enzymatic assay of δ^1-pyrroline-5-carboxylic acid. *Anal. Biochem.* **1975**, *64*, 85−97.
(27) Bradford, M. M. A rapid and sensitive method for the quantitation of microgram quantities of protein utilizing the principle of protein-dye binding. *Anal. Biochem.* **1976**, *72*, 248−254.
(28) Snedecor, G. W.; Cochran, W. G. *Statistical Methods*, 8th ed.; The Iowa State University Press: Ames, Iowa, 1989.
(29) Nocek, B.; Chang, C.; Li, H.; Lezondra, L.; Holzle, D.; Collart, F.; Joachimiak, A. Crystal structures of δ^1-pyrroline-5-carboxylate reductase from human pathogens *Neisseria meningitides* and *Streptococcus pyogenes*. *J. Mol. Biol.* **2005**, *354*, 91−106.
(30) Berman, H. M.; Westbrook, J.; Feng, Z.; Gilliland, G.; Bhat, T. N.; Weissig, H.; Shindyalov, I. N.; Bourne, P. E. The Protein Data Bank. *Nucleic Acids Res.* **2000**, *28*, 235−242.
(31) *Insight 2000, Molecular Modelling Program Package*; Accelrys: San Diego, CA, 2000.
(32) *DISCOVER, Molecular Modelling Program Package*; Accelrys: San Diego, CA, 2000.
(33) Böhm, H. J. The computer program LUDI: A new method for the de novo design of enzyme inhibitors. *J. Comput.-Aided Mol. Des.* **1992**, *6*, 61−78.
(34) Böhm, H. J. The development of a simple empirical scoring function to estimate the binding constant for a protein-ligand complex of known three-dimensional structure. *J. Comput.-Aided Mol. Des.* **1994**, *8*, 243−256.
(35) http://www.arabidopsis.org/.
(36) Murahama, M.; Yoshida, T.; Hayashi, F.; Ichino, T.; Sanada, Y.; Wada, K. Purification and characterization of δ^1-pyrroline-5-carboxylate reductase isoenzymes, indicating differential distribution in spinach (*Spinacia oleracea* L.) leaves. *Plant Cell Physiol.* **2001**, *42*, 742−750.
(37) Krueger, R.; Jager, H.-J.; Hintz, M.; Pahlich, E. Purification to homogeneity of pyrroline-5-carboxylate reductase of barley. *Plant Physiol.* **1986**, *80*, 142−144.
(38) Verbruggen, N.; Villarroel, R.; Van Montagu, M. Osmoregulation of a pyrroline-5-carboxylate reductase gene in *Arabidopsis thaliana*. *Plant Physiol.* **1993**, *103*, 771−781.
(39) Chilson, O. P.; Kelly-Chilson, A. E.; Siegel, N. R. Pyrroline-5-carboxylate reductase in soybean nodules: Isolation/partial primary structure/evidence for isozymes. *Arch. Biochem. Biophys.* **1991**, *288*, 350−357.
(40) Meng, Z.; Lou, Z.; Liu, Z.; Li, M.; Zhao, X.; Bartlam, M.; Rao, Z. Crystal structure of human pyrroline-5-carboxylate reductase. *J. Mol. Biol.* **2006**, *359*, 1364−1377.
(41) Forlani, G. Properties of the 5-*enol*-pyruvyl-shikimate-3-phosphate synthase isoforms isolated from maize cultured cells. *J. Plant Physiol.* **1997**, *150*, 369−375.
(42) Cascante, M.; Boros, L. G.; Comin-Anduix, B.; de Atauri, P.; Centelles, J. J.; Lee, P. W. Metabolic control analysis in drug discovery and disease. *Nat. Biotechnol.* **2002**, *20*, 243−249.

Received for review January 12, 2007. Revised manuscript March 23, 2007. Accepted March 23, 2007. Support from the University of Ferrara (Fondo d'Ateneo per la Ricerca 2006) is gratefully acknowledged.

JF0701032